An Arbitrage-free Interpolation of Volatilities

Nabil Kahalé [*]

May 14, 2003

Abstract

This paper presents a new interpolation method for implied volatilities in the equity and forex markets. If the market volatilities are arbitrage-free we compute an interpolating surface of the market volatilities for all strikes and maturities up to the last maturity that is arbitrage-free and satisfies some smoothness conditions. The basis block for our interpolation is a single-maturity interpolation with the following properties. If there are no absolute discrete dividends and the input volatilities are constant so are the interpolated volatilities. The second derivative of the call price with respect to the strike is positive and continuous, as shown by numerical experiments. The motivation for the second property is that the second derivative of the call price is proportional to the implied density of the spot. Our single-maturity interpolation does not depend on the shape of the discrete volatilities and applies to index, equity, forex and interest rate options. It takes seconds to calibrate a 10×10 volatilities matrix on a 800 Mhz processor and the quality of the fit is excellent. Using the regularity properties of the interpolated volatilities surface, local volatilities can be computed via Dupire's formula. This allows the pricing of exotic options, such as knock-out barrier options, by taking the smile into account. Numerical experiments show that prices of vanilla options computed via our local volatilities surface and a Crank-Nicholson scheme are very close to input prices. The local volatilities surface can be used to compute stable prices for exotic derivatives.

---

[*]Hiram Finance, 25 Rue d'Astorg, 75008 Paris. `nabil.kahale@hiram-finance.com`

1 Introduction

It is well known that the implied volatilities of quoted European options are non-constant and depend both on the strike and maturity of the option, a phenomenon is often referred to as the "smile". Various models have been proposed to explain and calibrate the smile (see [2, 3, 8, 4, 7, 5] and references therein.) Several problems arise in the presence of smile. First, arbitrage may exist among the quoted options. Another problem is to price European options for strikes and maturities not quoted on the market. Standard interpolation techniques may give rise to arbitrage in the interpolated volatilities surface even if there is no arbitrage in the original set. A related problem is to price non-vanilla options, such as barrier options, by taking the smile into account.

This paper presents a new interpolation method for implied volatilities. If the market volatilities are arbitrage-free we compute an interpolating surface of the market volatilities for all strikes and maturities up to the last maturity that is arbitrage-free and satisfies some smoothness conditions. The basis block for our interpolation is a single-maturity interpolation with the following properties (the first one holds only if there are no absolute discrete dividends):

- If the input volatilities are constant so are the interpolated volatilities.

- As shown by numerical experiments, the second derivative of the call price with respect to the strike is positive and continuous.

The motivation for the second property is that the second derivative of the call price is proportional to the implied density of the spot. One of the problems in finding an interpolation satisfying the above properties is that a standard smooth interpolation (such as the cubic interpolation) of a convexe function may not be convexe.

Our single-maturity interpolation does not depend on the shape of the discrete volatilities and applies to index, equity, forex and interest rate options. It takes seconds to calibrate a 10×10 volatilities matrix on a 800 Mhz processor and the quality of the fit is excellent. The interpolated volatilities surface can be used to calibrate Dupire's model [3]. This allows the pricing of exotic options, such as knock-out barrier options, by taking the smile into account, as described in Section 6. Numerical experiments show that prices of vanilla options computed via our local volatilities surface and a Crank-Nicholson scheme are very close to input prices.

The rest of this paper is organised as follows. Section 2 contains preliminary results. Section 3 gives an arbitrage-free one-dimensional interpolation which is provably C^1. Section 4 gives an arbitrage-free one-dimensional interpolation which numerical experiments show is C^2. Section 5 gives an overview of our two-dimensional interpolation algorithm. Section 2 through 6 assume we are in the equity market and there are no discount factors and no dividends. We point out how dividends and discount rates are taken into account in Section 7. An example on the S&P 500 index is given in Section 8. We show in Section 9 that our method can be used in the forex market and with some restrictions in the interest rate market (in the one-dimensional case). Section 10 contains concluding remarks.

2   Preliminaries

We use the following definition of arbitrage, which is slightly different from the one usually used in the litterature. We define an arbitrage as a self-financing portfolio of securities that has a negative value today and a nonnegative value at a given time in the future independently of the market behavior. Thus one is certain to make profit by buying such a portfolio.

It can been shown that if the input volatilities are given for all maturities and strikes there is no arbirage in the input if and only if the following conditions hold:

1. For a given maturity the call price is non-increasing and convexe with respect to the strike.

2. The call price is a non-decreasing function of time.

The convexity condition follows from the convexity of the payoff at maturity. Based upon this result one can find in linear time whether there exists an arbitrage within a discrete set of implied volatilities. In particular the following lemma can be shown in the one-dimensional case.

Lemma 1 *Consider a sequence $(k_i, c_i)_{0 \leq i \leq n+1}$ such that*

$$0 = c_{n+1} = k_0 < k_1 < \cdots < k_n < k_{n+1} = \infty \tag{1}$$

and c_i, $0 \leq i \leq n$, is the price of a call with strike k_i. There is no arbitrage among these prices if and only if c_0 is equal to the current spot and

$$-1 \leq \frac{c_i - c_{i-1}}{k_i - k_{i-1}} \leq \frac{c_{i+1} - c_i}{k_{i+1} - k_i} \leq 0 \text{ for } 1 \leq i \leq n. \tag{2}$$

3   A one-dimensional C^1 interpolation

We give in this section a C^1 arbitrage-free interpolation method for a given maturity. Like cubic interpolation, our method is based on the concatenation of several functions. Moreover, these functions are convex. Our construction is inspired from the Black-and-Scholes formula. We start with the following lemma:

Lemma 2 *For given $f > 0$, $\Sigma > 0$, a and b, the function*

$$c(k) = c_{f,\Sigma,a,b}(k) = fN(d_1) - kN(d_2) + ak + b, \tag{3}$$

defined for $k > 0$, where

$$d_1 = \frac{\log(f/k) + \Sigma^2/2}{\Sigma}$$

and $d_2 = d_1 - \Sigma$, is a convex function of k.

Proof: As in the Black-and-Scholes formula, we can check that the second derivative is positive using simple differentation:

$$c'(k) \quad = \quad -N(d_2) + a \tag{4}$$

$$c"(k) \quad = \quad \frac{N'(d_2)}{k\Sigma} \tag{5}$$

Lemma 3 *Let g be a real function defined for all real numbers such that $g'(x)$ exists and is positive for any real number x and $1/g'$ is strictly convex. For $\lambda \in]0, 1[$ and any real numbers $x_0 < x_1$, the function $h(a) = g(\lambda g^{-1}(a + x_0) + (1-\lambda)g^{-1}(a+x_1)) - a$ has a positive derivative with respect to a on the (possibly empty) interval on which it is defined.*

Proof: Let $y = g^{-1}(a + x_0)$ and $z = g^{-1}(a + x_1)$. By standard calculus

$$h'(a) = g'(\lambda y + (1 - \lambda)z)\left(\frac{\lambda}{g'(y)} + \frac{1-\lambda}{g'(z)}\right) - 1.$$

The equation $h'(a) > 0$ is equivalent to

$$\frac{\lambda}{g'(y)} + \frac{1-\lambda}{g'(z)} > \frac{1}{g'(\lambda y + (1-\lambda)z)},$$

which follows from the strict convexity of $1/g'$.

Theorem 1 *For all real numbers k_0, k_1, c_0, c_1, c_0', and c_1' such that $0 < k_0 < k_1$ and*

$$c_0' < \frac{c_1 - c_0}{k_1 - k_0} < c_1' < 1 + c_0' \tag{6}$$

there exists a unique vector (f, Σ, a, b) with $f > 0$, $\Sigma > 0$ such that the function $c = c_{f,\Sigma,a,b}$ satisfies the following conditions: $c(k_0) = c_0$, $c(k_1) = c_1$, $c'(k_0) = c_0'$ and $c'(k_1) = c_1'$. The vector (f, Σ, a, b) is continuous with respect to $(k_0, k_1, c_0, c_1, c_0', c_1')$ and can be computed numerically.

Proof: Given $a \in]c_1', 1 + c_0'[$, let d_2^0, d_2^1, α and β be the unique reals numbers such that

$$c_i' = -N(d_2^i) + a \tag{7}$$

and

$$d_2^i = \alpha \log(k_i) + \beta,$$

for $i \in \{0, 1\}$. The existence of d_2^i is a consequence of the inequalities $c_i' < a < c_i' + 1$ which follow from Eq. 6. Since $c_0' < c_1'$ we have $d_2^0 > d_2^1$ by Eq. 7, and thus

$$\alpha = \frac{d_2^0 - d_2^1}{\log(k_0) - \log(k_1)} < 0. \tag{8}$$

Hence there exist $f > 0$ and $\Sigma > 0$ such that $\alpha = -1/\Sigma$ and $\beta = (\log f)/\Sigma - \Sigma/2$. The following equation then holds:

$$d_2^i = \frac{\log(f/k_i) - \Sigma^2/2}{\Sigma}. \tag{9}$$

Note that d_2^i, α, β, f and Σ are continuous functions of a as a ranges in $]c_1', 1+c_0'[$. Consider the function $c = c_{f,\Sigma,a,b}$, where b is chosen so that $c(k_0) = c_0$. It follows from Eqs. 9 and 4 that $c'(k_i) = -N(d_2^i) + a$, and so $c'(k_i) = c_i'$ by Eq. 7. We now show that, for some $a \in]c_1', 1+c_0'[$, $c(k_1) = c_1$. The ratio $(c(k_1) - c(k_0))/(k_1 - k_0)$ is a continuous function of a. It follows from Eq. 4 that, for $k_0 < k < k_1$,

$$c'(k) = a - N(\lambda N^{-1}(a - c_0') + (1 - \lambda)N^{-1}(a - c_1')),$$

where $\lambda = \log(k_1/k)/\log(k_1/k_0)$. By applying Lemma 3 to the Normal function, we infer that $c'(k)$ is a strictly decreasing and has a negative derivative with respect to a. The same holds for the ratio $(c(k_1) - c(k_0))/(k_1 - k_0)$. When $a \to c_1'$, $c'(k) \to c_1'$ for $k \neq k_0$. It follows that

$$\frac{c(k_1) - c(k_0)}{k_1 - k_0} \to c_1' \text{ as } a \to c_1'.$$

Similarly,

$$\frac{c(k_1) - c(k_0)}{k_1 - k_0} \to c_0' \text{ as } a \to 1 + c_0'.$$

By continuity and Eq. 6, there exists $a_0 \in]c_1', 1 + c_0'[$ such that, for $a = a_0$,

$$\frac{c(k_1) - c(k_0)}{k_1 - k_0} = \frac{c_1 - c_0}{k_1 - k_0}.$$

Since $c(k_0) = c_0$, the equality $c(k_1) = c_1$ holds for $a = a_0$. Standard algorithms for inverting functions [6] can be used to compute a_0 numerically. The uniqueness and continuity of a_0 with respect to $(k_0, k_1, c_0, c_1, c_0', c_1')$ follows from the fact that the derivative of the ratio $(c(k_1) - c(k_0))/(k_1 - k_0)$ is negative with respect to a.

Lemma 4 *For all real numbers k_0, c_0, and c_0' such that $0 < k_0$, $-1 < c_0' < 0$ and $c_0 > 0$ there exist two unique parameters $f > 0$ and $\Sigma > 0$ such that the function $c = c_{f,\Sigma,0,0}$ satisfies the following conditions: $c(k_0) = c_0$, $c'(k_0) = c_0'$. Moreover $c(k) \to 0$ and $c'(k) \to 0$ as $k \to \infty$. The vector (f, Σ) is continuous with respect to (k_0, c_0, c_0') and can be computed numerically.*

Proof: Let d_2^0 be the unique real number such that $c_0' = -N(d_2^0)$. For $\Sigma > 0$, let $f = k_0 \exp(\Sigma d_2^0 + \Sigma^2/2)$. The function $c = c_{f,\Sigma,0,0}$ has a derivative equal to c_0' at k_0. As $\Sigma \to 0$, $c(k_0) \to 0$ and, as $\Sigma \to \infty$ $c(k_0) \to \infty$. Thus $c(k_0) = c_0$ when $\Sigma = \Sigma_0$, for some $\Sigma_0 > 0$. In order to show the uniqueness of Σ_0, we prove that $c(k_0)$ has a positive derivative with respect to Σ. Let $d_1 = d_2^0 + \Sigma$, so that $c(k_0) = fN(d_1) + k_0 c_0'$. The logarithmic derivative of $fN(d_1)$ with respect to Σ is $N'(d_1)/N(d_1) + d_1$, which is positive by standard calculus. The uniqueness and continuity of Σ_0 with respect to (k_0, c_0, c_0') follows. The calculation of the limits of $c(k)$ and $c'(k)$ as $k \to \infty$ follows by standard arguments.

Lemma 5 *For all real numbers k_1, c_0, c_1 and c_1' such that $0 < k_1$ and*

$$-1 < \frac{c_1 - c_0}{k_1} < c_1' < 0, \tag{10}$$

there exist three unique parameters $f > 0$ and $\Sigma > 0$ and b such that the function $c = c_{f,\Sigma,0,b}$ satisfies the following conditions: $c(k) \to c_0$ as $k \to 0$, $c'(k_1) = c_1'$, $c(k_1) = c_1$. Moreover, $c'(k) \to -1$ as $k \to 0$. the vector (f, Σ, b) is continuous with respect to (k_1, c_0, c_1, c_1') and can be computed numerically.

Proof: Let d_2^1 be the unique real number such that $c_1' = -N(d_2^1)$. For $\Sigma > 0$ let

$$f = k_1 \exp(\Sigma d_2^1 + \Sigma^2/2) \tag{11}$$

and

$$b = c_0 - f. \tag{12}$$

The function $c = c_{f,\Sigma,0,b}$ has a derivative equal to c'_1 at k_1. Moreover, $(c(k), c'(k)) \to (c_0, -1)$ as $k \to 0$ by standard calculations. It remains to show that $c(k_1) = c_1$ for some $\Sigma > 0$. Since $c(k_1) = fN(d_1) + k_1 c'_1 + b$, with $d_1 = d_2^1 + \Sigma$,

$$c(k_1) - c_0 = -fN(-d_2^1 - \Sigma) + k_1 c'_1 \tag{13}$$

by Eq. 12. Eq. 11 determines f as a function of Σ. As $\Sigma \to 0$, $f \to k_1$ and

$$c(k_1) - c_0 \to -k_1 N(-d_2^1) + k_1 c'_1 = -k_1.$$

Since $N(x) \sim N'(x)/|x|$ as $x \to -\infty$,

$$c(k_1) - c_0 \to k_1 c'_1 \text{ as } \Sigma \to \infty.$$

By continuity and Eq. 10 it follows that $c(k_1) = c_1$ when $\Sigma = \Sigma_0$, for some $\Sigma_0 > 0$. As in Lemma 4, it can be show that the derivative of $c(k_1)$ with respect to Σ is positive. This implies the uniqueness and continuity of Σ_0 with respect to (k_1, c_0, c_1, c'_1).

Combining Lemmas 2, 4, 5 and Theorem 1, we obtain the following theorem.

Theorem 2 *For all sequences $(k_i)_{0 \le i \le n+1}$, $(c_i)_{0 \le i \le n+1}$ and $(c'_i)_{0 \le i \le n+1}$ such that Eq. 1 holds together with the limit conditions*

$$c'_0 = -1, \ c'_{n+1} = 0, \tag{14}$$

and the convexity conditions

$$c'_i < \frac{c_{i+1} - c_i}{k_{i+1} - k_i} < c'_{i+1} \text{ for } 0 \le i \le n, \tag{15}$$

there exist a C^1 convex function $c(k)$, $k > 0$, and a unique sequence $(f_i, \Sigma_i, a_i, b_i)_{0 \le i \le n}$ such that $c(k) = c_{f_i, \Sigma_i, a_i, b_i}(k)$ on the interval $[k_i, k_{i+1}] - \{0, \infty\}$, $c(k_i) = c_i$ and $c'(k_i) = c'_i$ for $1 \le i \le n$. Moreover,

$$(c(k), c'(k)) \to (c_0, -1) \text{ as } k \to 0 \tag{16}$$

and

$$(c(k), c'(k)) \to (0, 0) \text{ as } k \to \infty. \tag{17}$$

The sequence $(f_i, \Sigma_i, a_i, b_i)_{0 \le i \le n}$ is continuous with respect to $(c_0, (k_i, c_i, c'_i)_{1 \le i \le n})$ and can be computed numerically.

There are $4(n+1)$ unknown parameters $(f_i, \Sigma_i, a_i, b_i)_{0 \le i \le n}$ that define the function c. Each equation $c(k_i) = c_i$, $1 \le i \le n$, accounts for two conditions on these parameters, because it holds both for $c_{f_i, \Sigma_i, a_i, b_i}(k_i)$ and $c_{f_{i-1}, \Sigma_{i-1}, a_{i-1}, b_{i-1}}(k_i)$. The same holds for the equation $c'(k_i) = c'_i$, $1 \le i \le n$. Together with the limit conditions as $k \to 0$ and as $k \to \infty$, there are $4n + 4$ conditions, which is equal to the number of parameters.

4 A C^2 interpolation method for a given maturity

The algorithm in Theorem 2 gives a C^1 convex interpolating curve for a given maturity. But, since the second of the call price with respect to the strike is proportional to the density of the strike in the risk-neutral word, a C^2 interpolating curve is desired. We give in this section an interpolating algorithm for the call prices for a given maturity which, based upon numerical experiments, we conjecture to converge towards a C^2 interpolating curve with the properties mentioned in Section 1. We start with a few lemmas to motivate our algorithm.

Lemma 6 *Let g be a convex C^1 function defined on the interval $[x_0, x_1]$, and $x_2 \in]x_0, x_1[$. The following holds:*

$$g'(x_1) - g'(x_2) \leq \eta \left(g'(x_1) - \frac{g(x_1) - g(x_0)}{x_1 - x_0} \right), \tag{18}$$

where $\eta = (x_1 - x_0)/(x_2 - x_0)$.

Proof: Since $g(x_2) - g(x_0) \leq g'(x_2)(x_2 - x_0)$ and $g(x_1) - g(x_2) \leq g'(x_1)(x_1 - x_2)$,
$$g(x_1) - g(x_0) \leq g'(x_2)(x_2 - x_0) + g'(x_1)(x_1 - x_2),$$

and so

$$g(x_1) - g(x_0) - g'(x_1)(x_1 - x_0) \leq (g'(x_2) - g'(x_1))(x_2 - x_0)$$

which is equivalent to Eq. 18.

Lemma 7 *For any $\gamma > 0$ there exists $\epsilon_0 > 0$ such that, for $\epsilon < \epsilon_0$, $\delta > 0$ and all u, if*
$$N(u + \delta) - N(u) < \epsilon \tag{19}$$
$$N(u + 2\delta) - N(u) > \gamma \tag{20}$$

then $\delta N'(u) < \epsilon$.

Proof: Assume without loss of generality that $\epsilon_0 < \gamma/2 < 1$. By Eq. 20, $N(u + 2\delta) - N(u + \delta) > \gamma/2$ and so

$$u + \delta < z_0, \tag{21}$$

where $z_0 = N^{-1}(1 - \gamma/2)$. Let $z \in [u, u + \delta]$ be such that $N(u + \delta) - N(u) = \delta N'(z)$. By Eq. 19,
$$\delta N'(z) < \epsilon. \tag{22}$$

Since the function N' is upper bounded by 1, it follows from Eq. 20 that $\delta > \gamma/2$, and so $N'(z) < 2\epsilon/\gamma$. But $z < z_0$ by Eq. 21. Let $\epsilon_0 = \gamma N'(z_0)/2$. If $\epsilon < \epsilon_0$ then $N'(z) < N'(z_0)$ and so $z < 0$. Hence $N'(u) \leq N'(z)$. By Eqs. 22 it follows that $\delta N'(u) < \epsilon$.

Lemma 8 *Given any real numbers k_0, k_1, c_0, c_1, c_0' such that $0 < k_0 < k_1$ and*

$$c_0' < \frac{c_1 - c_0}{k_1 - k_0} < 1 + c_0', \tag{23}$$

let $c_1' \in](c_1 - c_0)/(k_1 - k_0), 1 + c_0'[$ and (f, Σ, a, b) be the unique vector with $f > 0$, $\Sigma > 0$ such that the function $c = c_{f,\Sigma,a,b}$ satisfies the following conditions: $c(k_0) = c_0$, $c(k_1) = c_1$, $c'(k_0) = c_0'$ and $c'(k_1) = c_1'$. Then $c"(k_1) \to 0$ as $c_1' \to (c_1 - c_0)/(k_1 - k_0)$.

Proof: We show there exists $\epsilon_0, \theta > 0$ such that, for $0 < \epsilon < \epsilon_0$ if

$$\frac{c_1 - c_0}{k_1 - k_0} < c_1' < \frac{c_1 - c_0}{k_1 - k_0} + \epsilon$$

then $c"(k_1) < \theta\epsilon$. By chosing $\epsilon_0 < 1 + c_0' - (c_1 - c_0)/(k_1 - k_0)$, the existence of (f, Σ, a, b) follows from Theorem 1. Let $\gamma = (c_1 - c_0)/(k_1 - k_0) - c_0'$. By convexity $c'(k_1) - c'(k_0) > \gamma$. Using the same notation as in Theorem 1 and Eq. 4, it follows that

$$N(d_2^0) - N(d_2^1) > \gamma.$$

Let $k_2 = \sqrt{k_0 k_1}$. By Lemma 6, $c'(k_1) - c'(k_2) < \eta\epsilon$, where $\eta = (k_1 - k_0)/(k_2 - k_0)$. It follows that

$$N(\frac{d_2^0 + d_2^1}{2}) - N(d_2^1) < \eta\epsilon.$$

By Lemma 7, it follows that $(d_2^0 - d_2^1)N'(d_2^1) < 2\eta\epsilon$ for a suitable ϵ_0. Using Eq. 5, it follows after some calculations that $c"(k_1) < \theta\epsilon$, where $\theta = 2\eta/(k_1 \log(k_1/k_0))$.

Lemma 8 shows that $c"(k_1) \to 0$ as $c'(k_1)$ goes to its lower limit. Lemma 9 below shows a similar result holds in the limit case when $k_0 = 0$.

Lemma 9 *For all real numbers k_1, c_0 and c_1 such that $0 < k_1$ and*

$$-1 < \frac{c_1 - c_0}{k_1} < 0, \tag{24}$$

let c_1' range in $](c_1 - c_0)/k_1, 0[$ and $f > 0$, $\Sigma > 0$ and b be the three unique parameters such that the function $c = c_{f,\Sigma,0,b}$ satisfies the following conditions: $c(k) \to c_0$ as $k \to 0$, $c'(k_1) = c_1'$, $c(k_1) = c_1$. Then $c"(k_1) \to 0$ as $c_0' \to (c_1 - c_0)/k_1$.

Proof: We use the same notation as in Lemma 5, from which follows the existence of f, Σ and b. It follows from Eq. 13 that, as $c_0' \to (c_1 - c_0)/k_1$ $fN(-d_2^1 - \Sigma) \to 0$. Since, by Eq. 11 f is lower-bounded by $k_1 \exp(-(d_2^1)^2/2)$, it follows that $\Sigma \to \infty$. Thus $c"(k_0) \to 0$ by Eq. 5.

Lemma 10 *For all real numbers k_0, k_1, c_0, c_1, c_1' such that $0 < k_0 < k_1$ and*

$$c_1' - 1 < \frac{c_1 - c_0}{k_1 - k_0} < c_1' \tag{25}$$

there exists $\epsilon_0, \theta > 0$ such that, for $0 < \epsilon < \epsilon_0$ if

$$\frac{c_1 - c_0}{k_1 - k_0} - \epsilon < c_0' < \frac{c_1 - c_0}{k_1 - k_0},$$

there exists a unique vector (f, Σ, a, b) *with* $f > 0$, $\Sigma > 0$ *such that the function* $c = c_{f,\Sigma,a,b}$ *satisfies the following conditions:* $c(k_0) = c_0$, $c(k_1) = c_1$, $c'(k_0) = c'_0$, $c'(k_1) = c'_1$ *and* $c"(k_0) < \theta\epsilon$.

Proof: The proof is similar to the proof of Lemma 8 and is omitted.

Lemma 10 shows that $c"(k_0) \to 0$ as $c'(k_0)$ goes to its upper limit. Lemma 11 below shows a similar result holds in the limit case when $k_1 = \infty$.

Lemma 11 *For all real numbers* k_0, c_0 *such that* $0 < k_0$ *and* $c_0 > 0$, *let* c'_0 *range in* $]-1, 0[$ *and* $f > 0$ *and* $\Sigma > 0$ *be the two unique parameters such that the function* $c = c_{f,\Sigma,0,0}$ *satisfies the following conditions:* $c(k_0) = c_0$, $c'(k_0) = c'_0$. *Then* $c"(k_0) \to 0$ *as* $c'_0 \to 0$.

Proof: Using the same notation as in Lemma 4, standard algebra shows that, as $c'_0 \to 0$, $d_2^0 \to -\infty$, $fN(d_1) \to c_0$, $\Sigma \to \infty$, and thus $c"(k_0) \to 0$ by Eq. 5.

Theorem 3 *Let* j *be an integer in the interval* $[1, n]$. *For all sequences* $(k_i)_{0 \le i \le n+1}$, $(c_i)_{0 \le i \le n+1}$ *and* $(c'_i)_{0 \le i \le n+1}$ *such that Eqs. 1, 14 and 15 hold, there exist a* C^1 *convex function* $c(k)$, $k > 0$, *and a sequence* $(f_i, \Sigma_i, a_i, b_i)_{0 \le i \le n}$ *such that* $c(k) = c_{f_i,\Sigma_i,a_i,b_i}(k)$ *on the interval* $[k_i, k_{i+1}] - \{0, \infty\}$, $c(k_i) = c_i$ *for* $1 \le i \le n$, $c'(k_i) = c'_i$ *for* $1 \le i \le n$, $i \ne j$, *and* c *has a continuous second derivative at* k_j. *Moreover, the limit properties in Eqs. 16 and 17 hold. The sequence* $(f_i, \Sigma_i, a_i, b_i)_{0 \le i \le n}$ *can be computed numerically.*

Proof: For $1 \le i \le n$, let $l_i = (c_i - c_{i-1})/(k_i - k_{i-1})$. By Theorem 2, for any $\gamma \in]l_j, l_{j+1}[$, there exist a C^1 convex function $c(k)$, $k > 0$, and a sequence $(f_i, \Sigma_i, a_i, b_i)_{0 \le i \le n}$ such that $c(k) = c_{f_i,\Sigma_i,a_i,b_i}(k)$ on the interval $[k_i, k_{i+1}] - \{0, \infty\}$, $c(k_i) = c_i$ for $1 \le i \le n$, $c'(k_j) = \gamma$ and $c'(k_i) = c'_i$ for $1 \le i \le n$, $i \ne j$, and the limit conditions defined in Eqs. 16 and 17 hold. We show that for some $\gamma \in]l_j, l_{j+1}[$, c has a continuous second derivative at k_j.

As γ goes to l_j, the left second derivative $c"(k_j{}^-)$ of c at k_j goes to 0 by Lemmas 8 and 9. But the right second derivative $c"(k_j{}^+)$ of c at k_j goes to $c"_{f,\Sigma,a,b}(k_j)$, where the vector (f, Σ, a, b) is such that $c_{f,\Sigma,a,b}(k_j) = c_j$, $c'_{f,\Sigma,a,b}(k_j) = l_j$ and

$$(c_{f,\Sigma,a,b}(k), c'_{f,\Sigma,a,b}(k)) \to (c_{j+1}, c'_{j+1}) \text{ as } k \to k_{j+1}.$$

Hence, $c"(k_j{}^+) - c"(k_j{}^-)$ has a positive limit as γ goes to l_j. Similarly, it can be shown that $c"(k_j{}^+) - c"(k_j{}^-)$ has a negative limit as γ goes to l_{j+1}. By continuity, $c"(k_j{}^+) = c"(k_j{}^-)$ for some value of $\gamma \in]l_j, l_{j+1}[$.

As in Theorem 2, the number of constraints on the parameters is equal to the number of parameters in Theorem 3 because there are still four constraints at k_j: $c(k_j{}^+) = c(k_j{}^-) = c_j$, $c'(k_j{}^+) = c'(k_j{}^-)$ and $c"(k_j{}^+) = c"(k_j{}^-)$. Unlike Theorem 2, though, it is not clear whether the function constructed in Theorem 3 is unique.

4.1 Algorithm description

We are now ready to describe our algorithm. Consider a sequence $(k_i)_{0 \le i \le n+1}$, $(c_i)_{0 \le i \le n+1}$ and such that Eq. 1 holds and

$$-1 < \frac{c_i - c_{i-1}}{k_i - k_{i-1}} < \frac{c_{i+1} - c_i}{k_{i+1} - k_i} < 0 \text{ for } 1 \le i \le n. \tag{26}$$

Note that Eq. 26 is the same as Eq. 2 except that inequalities have been replaced by strict inequalities. Let $\epsilon > 0$ be an error parameter. Algorithm A consists of the following procedures:

1. Initialization Step. Let $c'_0 = -1$, $c'_{n+1} = \infty$ and $c'_i = (l_i + l_{i+1})/2$, for $1 \le i \le n$, where $l_i = (c_i - c_{i-1})/(k_i - k_{i-1})$.

2. Loop. For $1 \le j \le n$, let $\gamma_j = c'_j(k_j)$, where c_j is a function calculated in Theorem 3 for the index j. Replace simultaneously (c'_j) by γ_j, $1 \le j \le n$. Repeat this step until $\max_{1 \le j \le n}(|c"(k_j{}^+) - c"(k_j{}^-)|) < \epsilon$.

Conjecture 1 *For all sequences $(k_i)_{0 \le i \le n+1}$, $(c_i)_{0 \le i \le n+1}$ such that Eqs. 1, and 26 hold, the sequences computed by Algorithm A converge in the limit towards a sequence $(f_i, \Sigma_i, a_i, b_i)_{0 \le i \le n}$. There exists a C^2 convex function $c(k)$, $k > 0$, such that $c(k) = c_{f_i, \Sigma_i, a_i, b_i}(k)$ on the interval $[k_i, k_{i+1}] - \{0, \infty\}$ and $c(k_i) = c_i$ for $1 \le i \le n$. Moreover, the limit properties in Eqs. 16 and 17 hold.*

The number of constraints on the parameters in Congecture 1 is equal to the number of parameters. To see this, we note there are still four constraints at k_j, $1 \le j \le n$: $c(k_j{}^+) = c(k_j{}^-) = c_j$, $c'(k_j{}^+) = c'(k_j{}^-)$ and $c"(k_j{}^+) = c"(k_j{}^-)$. Since there are four limit constraints by Eq. 17, the total number of constraints is equal to $4n + 4$, which is equal to the number of parameters. It is not clear, though, whether there exists a unique function c satisfying the properties in Congecture 1.

Several tricks can be used to improve the numerical stability and speed of convergence of Algorithm A. We tested a variant of Algorithm A on various inputs. Our experiments support Conjecture 1.

5 Interpolating the volatilities

If no arbitrage is found in the input volatilities, our algorithm generates an arbitrage-free interpolating volatilities surface as follows:

1. It generates a one-dimensional arbitrage-free interpolation for each input maturity t_i using a variant of Algorithm A.

2. For each maturity $t \in]t_i, t_{i+1}[$ and each strike K, calculate the implied volatility $\sigma(K, t)$ so that $\sigma^2(K, t)t$ is a linear interpolation of $\sigma^2(K, t_i)t_i$ and $\sigma^2(K, t_{i+1})t_{i+1}$.

3. Make the necessary adjustments so that the entire volatilities surface is arbitrage-free.

Because of the adjustments made in the last step, the smoothness properties of the one-dimensional interpolation described in Section 1 may not hold for the two-dimensional interpolation. However, numerical experiments in the two-dimensional case show that, for any maturity up to the last input maturity, the second derivative of the call price with respect to the strike exists and is continuous and positive except for a few points. Moreover, the derivative with respect to time is continuous except at input maturities. These properties help to ensure the stability of pricing exotic options using Dupire's model.

6   Calibrating Dupire's Model

In Dupire's model [3] the spot has a local volatility that depends both on the current time and current spot. More precisely, the spot follows the following stochastic differential equation:

$$dS_t = \mu_t S_t dt + \sigma(S_t, t) S_t dW_t,$$

where W_t is a Brownian motion and $\sigma(S, t)$ is a deterministic function. Dupire has shown that if the implied volatilities are known for all strikes and maturities then the local volatilities surface is uniquely determined. More precisely,

$$\sigma^2(K, t) = 2 \frac{\frac{\partial C(K,T)}{\partial T}}{K^2 \frac{\partial^2 C(K,T)}{\partial K^2}},$$

where $C(K, T)$ is today's price of a European call with strike K and maturity T. Several pros and cons of Dupire's model can be found in the litterature. A classical problem in implementing the model is the instability of the local volatilities calculation. According to the practical cases we tested our interpolating algorithm is well suited to calibrating Dupire's model. This is because, in practice, the second derivative of the call with respect to the strike exists and is continuous and positive for maturities up to the last input maturity, as mentionned in Section 5. Moreover the call derivative with respect to the maturity exists and is continuous and positive except at input maturities, where the left and right derivatives are different. The local volatility is therefore continuous except at input maturities, and can be computed approximatly using finite difference approximations of derivatives.

It is known that the price of a contingent claim on S obeys the following PDE:

$$\frac{\partial C(S,t)}{\partial t} + \frac{1}{2}\sigma^2(S,t)S^2\frac{\partial^2 C(S,t)}{\partial S^2} = 0.$$

where $C(S, t)$ is the price at time t of a contingent claim if the spot price is S at time t. We can therefore use the local volatilities surface to compute option prices using finite difference schemes such as the Crank-Nicholson algorithm. The local volatility is not continuous at input maturities but this does not cause a problem in implementing a finite difference algorithm.

7   Dealing with dividends and discount factors

Discount factors and continuous dividends can be taken care of by introducing additional terms in the previous equations that depend on the derivative of

T \ K	85%	90%	95%	100%	105%	110%	115%	120%	130%	140%
0.175	0.190	0.168	0.133	0.113	0.102	0.097	0.120	0.142	0.169	0.200
0.425	0.177	0.155	0.138	0.125	0.109	0.103	0.100	0.114	0.130	0.150
0.695	0.172	0.157	0.144	0.133	0.118	0.104	0.100	0.101	0.108	0.124
0.940	0.171	0.159	0.149	0.137	0.127	0.113	0.106	0.103	0.100	0.110
1.000	0.171	0.159	0.150	0.138	0.128	0.115	0.107	0.103	0.099	0.108
1.500	0.169	0.160	0.151	0.142	0.133	0.124	0.119	0.113	0.107	0.102
2.000	0.169	0.161	0.153	0.145	0.137	0.130	0.126	0.119	0.115	0.111
3.000	0.168	0.161	0.155	0.149	0.143	0.137	0.133	0.128	0.124	0.123
4.000	0.168	0.162	0.157	0.152	0.148	0.143	0.139	0.135	0.130	0.128
5.000	0.168	0.164	0.159	0.154	0.151	0.148	0.144	0.140	0.136	0.132

Figure 1: Implied volatilities surface on the S&P 500 index on October 1995. The maturity T is expressed in years and the strike K as a percentage of the initial spot $S_0 = \$590$. The interest rate is $r = 6\%$ and the dividend yield is $q = 2.62\%$.

the call price with respect to the strike. Absolute dividends and dividends in percentage are more problematic. In general, by arbitrage, volatility can no longer be a continuous function of the strike at dividend dates. For the same reason volatility cannot be constant everywhere in the presence of absolute dividends. Our algorithm can be adapted to generate an arbitrage-free implied volatilities surface that has the same smoothness properties mentionned in the preceding sections except at discrete dividend dates. Local volatilities can still be used to recover input prices but the error rate of the computed prices is generally higher.

8 Example

Fig. 1 shows the implied volatilities matrix of the S&P 500 index on October 1995 given in [1].

We plot in Fig. 2 the interpolated volatilities surface, in Fig. 3 the call price, in Fig. 4 the risk-neutral density function of the spot, and in Fig. 5 the local volatilities surface.

In Fig. 6 we compare the two-years call Black-and-Scholes prices using the interpolated volatilities and the input volatilities to the prices computed using the local volatilities surface (via a Crank-Nicholson scheme with 100 time-steps). The maximum difference is about 6 cents. Fig. 7 shows the relative errors (differences divided by the initial spot) between all input prices and the prices obtained via the Crank-Nicholson scheme together with our local volatilities surface. Fig. 8 shows the relative errors between all input prices and the prices obtained via Monte Carlo simulation together with our local volatilities surface. Numerical experiments show that prices of knock-out barrier options using our local volatilities surface are stable in terms of the spot, number of time-steps, and barriers levels.

9 The foreign exchange and interest rate markets

Our algorithm can readily be used in the foreign exchange derivatives market because the foreign exchange dynamics are similar to the equity dynamics. The
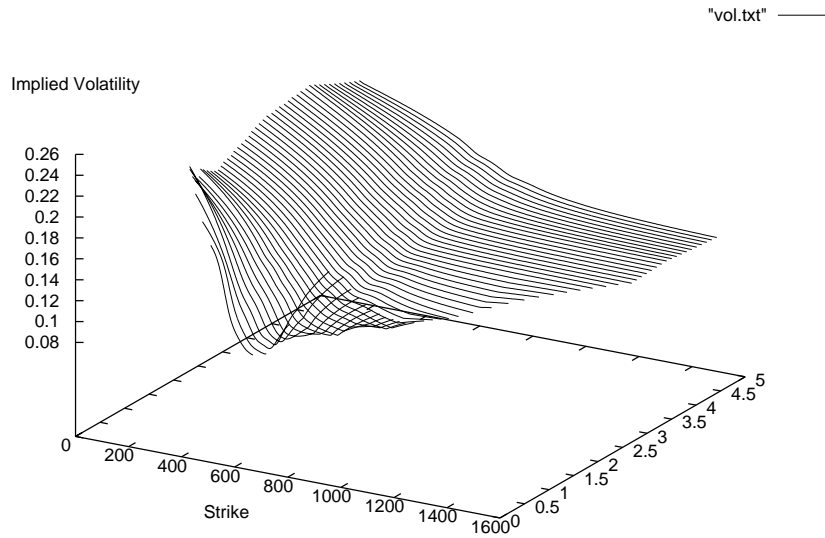
Figure 2: Interpolated Implied volatilities on the S&P 500 index on October 1995 in terms of the maturity and the strike.
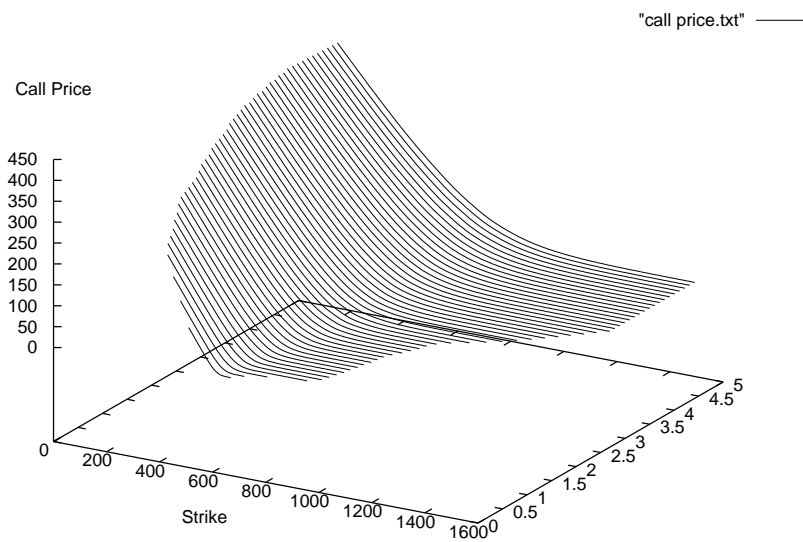

Figure 3: Call price on the S&P 500 index on October 1995 in terms of the maturity and the strike.
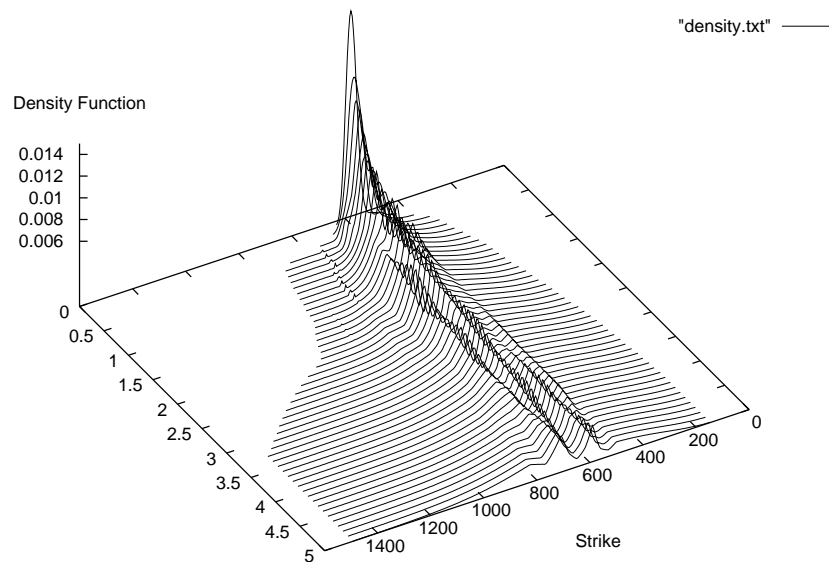
Figure 4: Implied risk-neutral density function of the spot of the S&P 500 index on October 1995 in terms of the maturity and the strike.
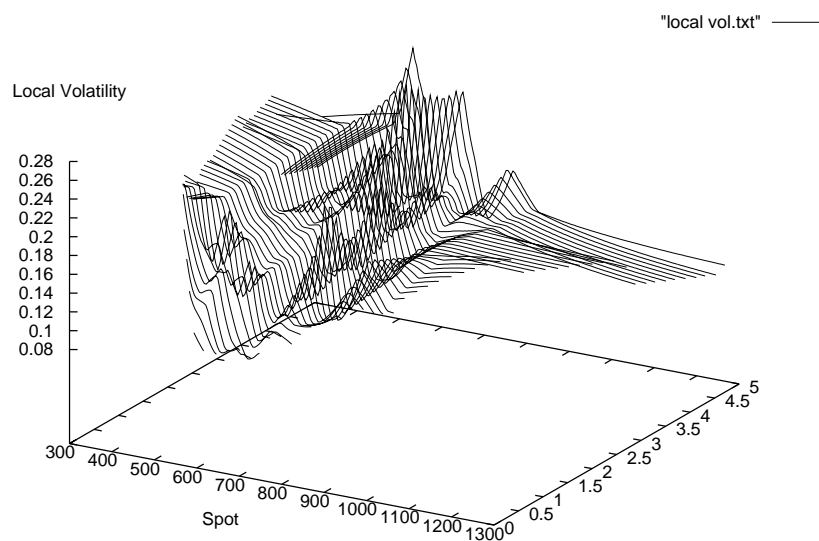

Figure 5: Local volatilities on the S&P 500 index on October 1995 in terms of the time and spot.

Strike in %	BS input price	BS interpolated price	Finite diff. price
85	125, 7023	125, 7023	125, 6992
90	103, 9506	103, 9506	103, 9517
95	83, 5822	83, 5821	83, 5801
100	64, 8987	64, 8987	64, 8965
105	48, 2225	48, 2226	48, 2127
110	34, 1869	34, 1870	34, 2147
115	23, 6128	23, 6124	23, 5570
120	14, 6757	14, 6760	14, 6960
130	5, 6466	5, 6465	5, 6157
140	1, 7778	1, 7779	1, 7569

Figure 6: Two-years call Black-and-Scholes prices using the input volatilities, the interpolated volatilities and the finite difference Crank-Nicholson prices using 100 time-steps on the S&P 500 index on October 1995.
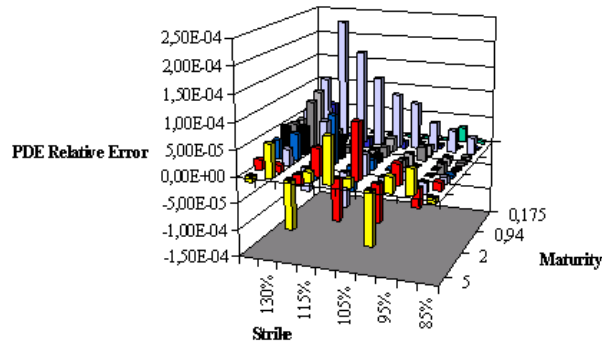

Figure 7: Relative errors on call prices of the S&P 500 index on October 1995 using our local volatilities surface together with the Crank-Nicholson PDE method, with 100 time-steps and 1000 space steps.
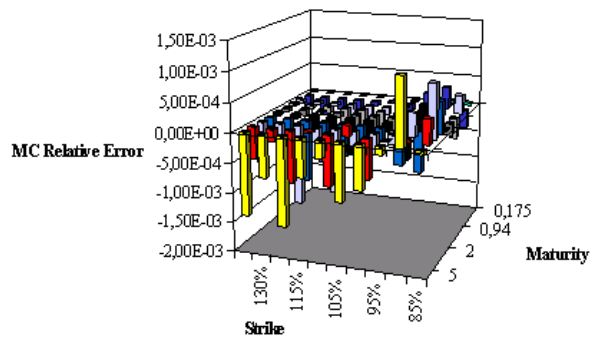
Figure 8: Relative errors on call prices of the S&P 500 index on October 1995 using our local volatilities surface together with the Monte Carlo method, with 100 time-steps and 10^5 samples.

continuous dividend rate is simply replaced by the foreign exchange rate.

Our one-dimensional algorithm can be used to interpolate volatilities on options expiring at a given maturity T on a swap or interest rate spanning a given period I. A slight modification is needed however if we assume the interest rates can be negative.

10 Conclusion

We have developped a one-dimensional interpolation algorithm for implied volatilities that is robust and has good smoothness properties. Our algorithm can be extended to the two-dimensional case. In practice the regularity properties of our interpolation ensure it can be used to calibrate Dupire's model. The local volatilities surface produced by our algorithm give stable prices for exotic options such as barrier options in a way consistent with quoted plain-vanilla options.

References

[1] L. B. G. Andersen and R. Brotherton-Ratcliffe. The equity option volatility smile: an implicit finite-difference approach. *Journal Of Computational Finance*, 1(2):5–37, 1998.

[2] E. Derman and I. Kani. Riding on a smile. *Risk*, 7(2):32–39, 1994.

[3] B. Dupire. Pricing with a smile. *Risk*, 7(7):18–20, 1994.

[4] R. Lagnado and S. Osher. A technique for calibrating derivative security pricing models: numerical solution of an inverse problem. *Journal of Computational Finance*, 1(1):13–25, 1997.

[5] Y. Li. A new algorithm for constructing implied binomial trees: does the implied model fit any volatility smile? *Journal of Computational Finance*, 4(2):69–95, 2001.

[6] William H. Press, Brian P. Flannery, Saul A. Teukolsky, and William T. Vetterling. *Numerical Recipes in C : The Art of Scientific Computing*. Cambridge University Press, 1993.

[7] R. Rebonato. *Volatility and Correlation*. Wiley, 1999.

[8] M. Rubinstein. Implied binomial trees. *Journal of Finance*, 49:771–818, 1994.